Hindawi Publishing Corporation
International Journal of Corrosion
Volume 2014, Article ID 707465, 7 pages
http://dx.doi.org/10.1155/2014/707465

Research Article

Exploratory Study of Sensitization in Cryogenically Cooled Ferritic Stainless Steel Welds

M. O. H. Amuda[1,2] and S. Mridha[2,3]

[1] *Materials Development and Processing Research Group, Department of Metallurgical and Materials Engineering, University of Lagos, Lagos 101017, Nigeria*
[2] *Advanced Materials and Surface Engineering Research Unit, Department of Manufacturing and Materials Engineering, International Islamic University Malaysia, P.O. Box 10, 50728 Kuala Lumpur, Malaysia*
[3] *Department of Mechanical and Aerospace Engineering, Strathclyde University, Glasgow G1 1XJ, UK*

Correspondence should be addressed to M. O. H. Amuda; mamuda@unilag.edu.ng

Received 15 July 2014; Accepted 12 November 2014; Published 7 December 2014

Academic Editor: Aravamudhan Raman

Enhanced cooling via forced convection using cryogenic liquid is an option for controlling grain growth in the heat affected zone (HAZ) of ferritic stainless steel welds which improves joint strength. However, this technique seems to alter the martensite distribution in the high-temperature heat affected zone (HTHAZ) which is a critical constituent in rating the susceptibility to sensitization in ferritic stainless steel grades; any such information is not available in the literature. Thus, it is imperative to establish the influence of cryogenic cooling on sensitization dynamics in the HTHAZ. This paper discusses the influence of cryogenic cooling on sensitization in an AISI 430 ferritic stainless steel weld. It is established that cryogenic cooling increases the cooling rate in the HTHAZ and reduces the martensite volume percent by an average of 20%. This reduction in martensite content in the HTHAZ increases the level of ditched structure in cryogenically cooled welds and yields more ferrite-martensite ditched grain boundaries than in conventional welds. Although the cryotreated welds exhibit greater ditched boundary, the structure is still classified as nonsensitized, since no single grain boundary is completely surrounded by ditches.

1. Introduction

Ferritic stainless steels are credited with better stress corrosion cracking resistance as well as superior resistance to pitting and crevice corrosion in chloride environment than the austenitic varieties [1–3]. They also have additional property advantages over the austenitics in such areas as improved machinability, higher thermal conductivity, and lower thermal expansion [4]. These grades provide a cost saving of approximately one-half of one percent over the austenitic grades and are, as such, attractive alternatives to the austenitics [5]. The ferritics are, however, hitherto rarely used in engineering application because welding is known to reduce their toughness and ductility [6]. This is more pronounced in the first generation ferritics like the medium chromium ferritic grade containing a maximum of 0.12 wt.% carbon and 15–18 wt.% chromium. The reduction in the properties is attributed to intense grain coarsening in the weld section caused by the heat input and cooling dynamics during the welding process. The reduction in ductility and toughness in the ferritic stainless steel weld is aggravated by the loss in corrosion resistance in regions around the weld section, particularly those adjacent to the weld interface, referred to as the HTHAZ which have been heated to temperatures in the region of 950°C during the weld thermal cycle [4]. The ferritic stainless steel weld in this condition is said to be sensitized and represents a state in which the steel is greatly susceptible to intergranular corrosion and eventually stress corrosion cracking [7–10]. This condition is due to the presence of chromium depleted zones at the grain boundary [9].

Different welding techniques have been adopted to control grain coarsening in ferritic stainless steel welds with the focus of controlling the heat input and its transfer dynamics

during the welding process [11]. In furtherance of this effort, Amuda and Mridha [12] reported the adoption of cryogenic cooling via enhanced convective flow of liquid nitrogen for the control of the grain structure of AISI 430 ferritic stainless steel welds. The study indicated that cryogenic weld cooling can achieve up to 40% grain refinement in the weld section. However, the study on the influence of this strategy on sensitization in the ferritic stainless steel weld is yet to be undertaken. The use of cryogenic cooling probably alters the martensite content in the HTHAZ which is a critical constituent in determining the susceptibility to sensitization in ferritic stainless steel grades [4, 13]. Therefore, in the present paper, an exploratory study of the influence of cryogenic cooling on the sensitization behaviour in medium chromium ferritic stainless steel welds corresponding to the commercial grade AISI 430 is reported. It is expected that the current effort will provide an insight into the effect of enhanced convection cooling on the susceptibility to intergranular corrosion in the weld of this grade of ferritic stainless steel.

2. Materials and Method

Annealed cold-rolled plates, 1.5 mm thick, were cut from a 1 m × 1 m AISI 430 ferritic stainless steel plate into required test dimensions of size 65 mm × 25 mm using a Sunfluid hydraulic shearing machine, model 300 D/10. The chemical composition of the base metal provided by the supplier and complemented with energy dispersive X-ray fluorescence spectroscopy is given in Table 1. The Kaltenhauser ferrite factor (KFF), calculated from (1), is also included in the table. The factor gives a range of numerical values for the likelihood of sensitization in different grades of ferritic stainless steel [14]:

$$\begin{aligned} \mathrm{KFF} = {} & \mathrm{Cr} + 6\mathrm{Si} + 8\mathrm{Ti} + 4\mathrm{Mo} + 2\mathrm{Al} \\ & - 40\left((\mathrm{C} + \mathrm{N}) - 2\mathrm{Mn} - 4\mathrm{Ni}\right) \text{ wt.\%}. \end{aligned} \tag{1}$$

In order to examine the influence of enhanced convection via cryogenic cooling on the microstructure and sensitization resistance of the HTHAZ adjacent to the weld interface three different heat input conditions were considered at a welding current of 90 A and welding speeds of 1, 2.5, and 3.5 mm/s, respectively, using a constant arc voltage of 30 V. Two streams of weld tracks were produced; one group of track was produced on samples exposed to direct liquid nitrogen after welding while the other stream produced and cooled under normal condition served as the control weld tracks for the investigation. Thus, a total of six weld samples were produced. The melting conditions used for the investigation are provided in Table 2.

Direct current negative polarity for the electrode with argon shielding at a flow rate of 0.72 L/min was used. The electrode negative polarity adopted focused most of the welding heat into the workpiece and restricted the electrode heating thereby minimizing heat losses through the tungsten electrode. The actual heat input into the workpiece was calculated using (2) proposed by Easterling [15]:

$$\mathrm{HI} = \frac{\eta V I}{\nu}, \tag{2}$$

where η = efficiency, I = current in A, V = voltage, and ν = welding speed in mm/s.

Transverse samples for metallographic analysis and sensitization test were wire-cut from the weld specimen using electric discharge machining (EDM). The samples were ground to 1000 grit size and polished to mirror finish using 1 μm alpha agglomerated alumina suspension paste. Sensitization was evaluated using 10% oxalic acid electrolyte as described in practice W, ASTM A763-93 [16]; the samples were subsequently examined under Nikon Epiphot model 200 Metallurgical Microscope incorporated with image analysis software to determine the volume fraction of martensite in each weld.

The time required for a point on the weld interface to cool from 1500° to 800°C, $\Delta t_{15/8}$, was calculated from (3) based on Rosenthal conduction heat flow model for thin plates [17]:

$$\Delta t_{15/8} = \frac{(q/\nu)^2}{4\pi\lambda\rho c d^2 \theta_2}, \tag{3}$$

where q is the heat flux (W), λ is thermal conductivity of AISI 430 ferritic stainless steel (J/s/m/°C), ρc is the specific heat capacity per unit volume (J/m^3/°C), d is the thickness of the material (mm), and θ_2 is the dimensionless thermal gradient associated with the process.

Table 1: Chemical composition of AISI 430 ferritic stainless steel (% by mass, balance Fe).

Material spec.	Composition						KFF
	C	Cr	Si	Mn	P	S	
AISI 430	0.12	16.19	0.75	1.0	0.04	0.30	14.7

Table 2: Melting conditions.

Process	DCEN straight polarity full bead on plate penetration GTA weld
Position	Flat
Melting conditions	
Current	90 A
Voltage	30 V
Speed	1, 2.5, 3.5 mm/s
Arc length	1.5 mm
Torch orientation	Vertical
Electrode configuration	2.44 mm W-2 pct. Th., 60° cone included angle
Electrode stick-out	3 mm
Cryogenic coolant	Liquid nitrogen
Shielding environment	99.9% argon at a flow rate of 0.72 L/min

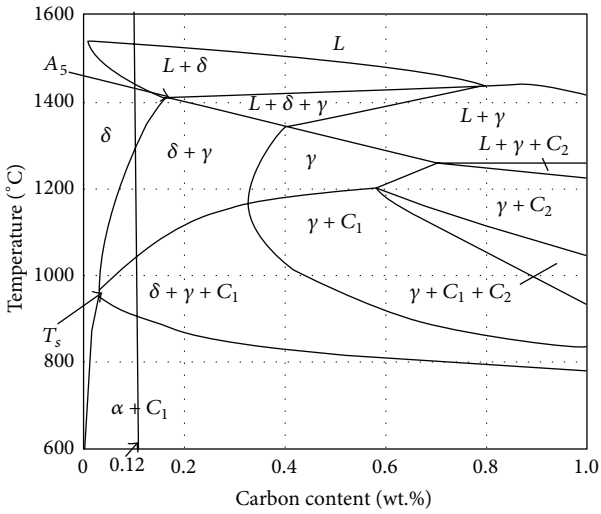

Figure 1: Vertical section of the Fe–Cr–C-ternary diagram at 17 wt.% Cr [4].

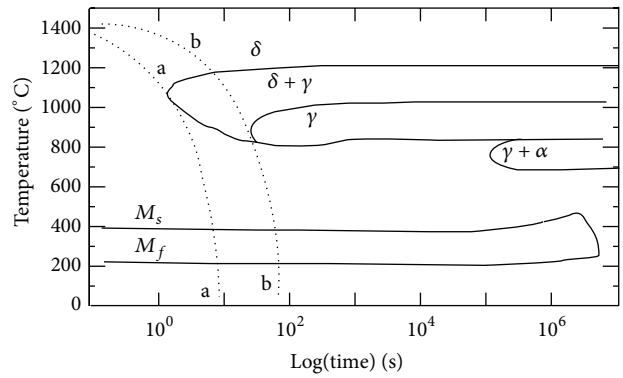

Figure 2: Continuous cooling transformation of δ-ferrite to γ in the HTHAZ during weld thermal cycle [18].

The cooling time was then used to estimate the cooling rate (T') experienced by that point of the HTHAZ with the following equation:

$$T'_{15/8} = \frac{700}{\Delta t_{15/8}}. \quad (4)$$

The 1500°–800°C temperature range represents the interval from the liquidus point to points just below the austenite phase field, as shown in Figure 1; thus, it includes the range for the solid state transformation of δ-ferrite to austenite.

3. Results and Discussion

The compositional analysis of the ferritic stainless steel material stated in Table 1 shows that the material belongs to medium chromium grade with 0.12 wt.% carbon. The vertical section of the Fe–Cr–C ternary diagram for this grade of ferritic stainless steel, shown in Figure 1, indicates that, with 0.12 wt.% C, under equilibrium cooling, the steel will transform partially to austenite from the A_5 temperature, passing through the $\delta + \gamma$ dual phase region until the austenite transformation temperature (T_s) is reached. Beyond this temperature, the austenite transforms to ferrite. This ambient temperature ferrite is supersaturated in carbon; therefore, the excess carbon is precipitated as chromium carbide which promotes intergranular corrosion when in hostile environment [4]. However, in fusion welding, the cooling sequence is far-off of equilibrium mechanism; it involves very rapid cooling rates.

Therefore, any austenite formed on cooling through the $\delta+\gamma$ dual phase region transforms to martensite below the M_s temperature, shown in Figure 2, which illustrates the typical cooling sequence from δ-ferrite to γ in the HTHAZ. Path aa in the figure approximates the cooling sequence in a welding process while bb represents that in equilibrium cooling. Consequently, the microstructure of the HTHAZ closest to the weld interface consists of ferrite matrix surrounded by a network of grain boundary martensite. The KFF value as calculated from (1) and listed in Table 1 equally predicts the presence of martensite in the HTHAZ on cooling to lower temperature.

The optical microstructure of the HTHAZ of the weld section is shown in Figure 3. The figure reveals two-phase ferrite matrix networked by grain boundary martensite. The martensite formed from the elevated temperature austenite acts as carbon sinks, taking significant amount of carbon into solution. However, the amount of carbon retained in solution in ferrite depends on the volume percent of martensite which is determined by the heat input and cooling rates.

The martensite content in the HTHAZ of the welds was measured using point counting technique and the result is shown in Figure 4. The figure reveals that the martensite content in the zone increases as the heat input increases. However, cryogenic weld cooling leads to a reduction in the martensite content. The increase in the martensite content with increase in heat input is due to the reduction in cooling rate associated with higher heat input particularly at 1290 J/mm which allows longer time at the $\delta + \gamma$ dual phase region. This encourages the formation of more elevated temperature austenite which eventually transforms to martensite once the M_s temperature is crossed [19]. This postulation has equally been reported by Glover et al. [20] as being responsible for the presence of more martensite in the weld metal during cooling from elevated temperature.

On the contrary, with cryogenic weld cooling, the cooling rate increased not from reduction in the heat input but due to the convective effect of the liquid nitrogen which shortens the time spent in the dual phase region and inhibits the transformation of delta-ferrite to austenite. The reduction in the amount of elevated temperature austenite correspondingly leads to a reduction by about 20% in the martensite content in the HTHAZ, irrespective of the heat input.

The influence of heat input and cryogenic cooling on the cooling rate experienced by the HTHAZ is shown in Figure 5. The figure demonstrates that as the heat input increases the cooling rate decreases. The figure equally shows that, at the same level of heat input, cryocooled welds experience

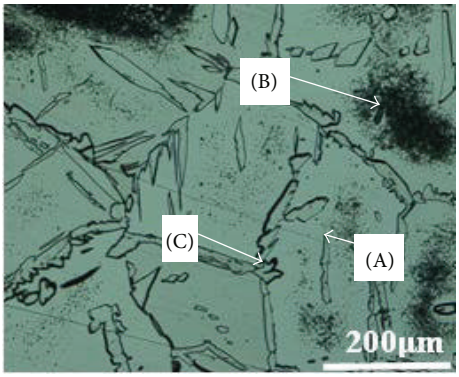

Figure 3: Optical microstructure of the HTHAZ of the weld section (A-α-ferrite, B-δ-ferrite, and C-martensite).

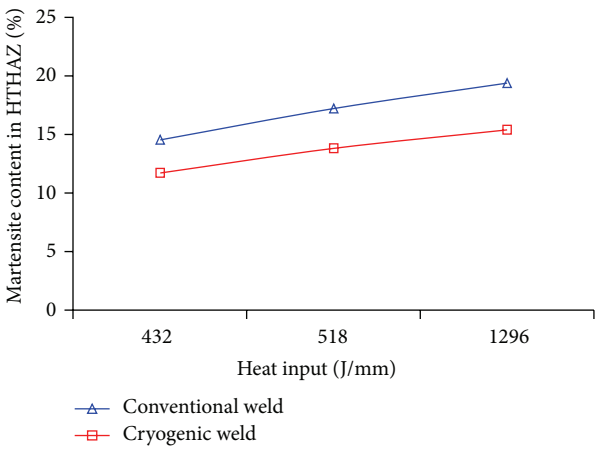

Figure 4: Martensite content in HTHAZ of the welds as a function of heat input and cooling conditions.

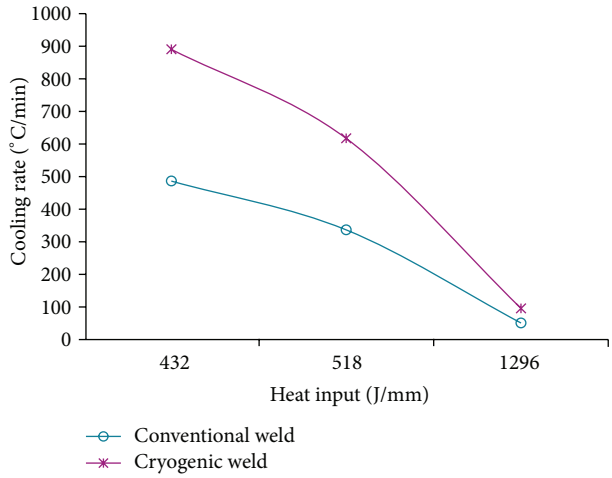

Figure 5: Combined effect of heat input and cooling conditions on the cooling rate from 1500 to 800°C at a point in the HTHAZ adjacent to the weld interface.

Table 3: Classification of etched structure in oxalic acid electrolytic etch [16].

Classification	State of the microstructure
Acceptable	(i) *Step structure*: step only between grains, no ditches at the grain boundary (ii) *Dual structure*: some ditches at the grain boundary in addition to steps; however, no single grain is completely surrounded by ditches
Unacceptable	*Ditch structure*: one or more grains are completely surrounded by ditches

higher cooling rates, almost two-fold that of the conventional welds. This will, obviously, influence the transformation in the dual phase region and account for the relative change in the martensite content shown in Figure 4. However, the wide difference between the cooling rates experienced by the cryogenically cooled welds and conventional welds reduces as the heat input increases and drops to around 100°C/min at 1296 J/mm.

But this convergence of cooling rates at 1296 J/mm does not seem to have any significant effect on the volume of martensite in the HTHAZ at this particular heat input.

The etched structures in oxalic acid electrolytic test method are classified in Practice W, ASTM A763-93 as either acceptable or unacceptable, depending on the state of the grain boundary. The detail of the classification is summarized in Table 3. This classification is used to screen the etched microstructure in the HTHAZ of the weld section for susceptibility to intergranular attack.

The microstructures of the HTHAZs at various conditions of heat input without and with cryogenic cooling, etched electrolytically in 10% oxalic acid at 6 V for 60 s, are presented in Figures 6 and 7, respectively. The etched microstructures of Figure 6 show partial and discontinuous ditches at the grain boundaries. However as the heat input increases fewer grain boundaries exhibit ditched structure. At 432 J/mm, about 37% of the grain boundary is ditched and this reduces to less than 20% at 1290 J/mm. Furthermore, the ditches occur on the ferrite-ferrite grain boundary, whereas intermittent attack is apparent on the ferrite-martensite interface.

Figure 7 shows that, in cryogenically cooled welds, more grain boundaries are ditched for the same level of heat input relative to conventional welds. The ditched grain boundary increases in these welds from 21% to 65% at 432 and 1296 J/mm, respectively. More significant is the observation that more ditches occur on the ferrite-martensite grain boundaries than in conventional welds. The arrow in the microstructures points to the ditched boundaries in the two welds. The microstructure is generally acceptable based on the ASTM Standard A763-93 since no single grain is completely surrounded by ditches as classified by the conditions listed in Table 3, although the cryogenically cooled welds present higher level of ditches relative to those of conventional welds.

The degree of ditching observed in this study is a function of the metallurgical phase balance in the HTHAZ due to

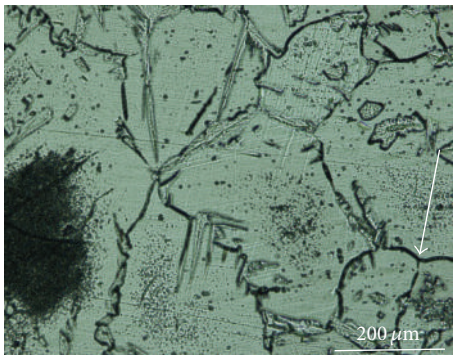

(a) 423 J/mm

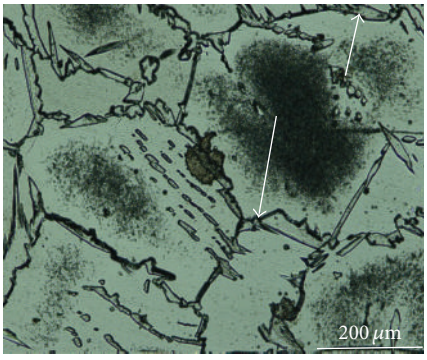

(b) 518 J/mm

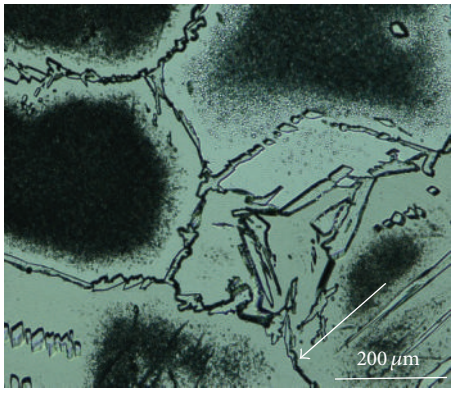

(c) 1296 J/mm

Figure 6: Microstructure of HTHAZ of conventional weld etched electrolytically in 10% oxalic acid.

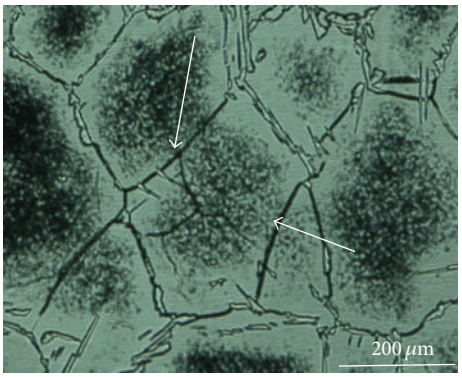

(a) 423 J/mm

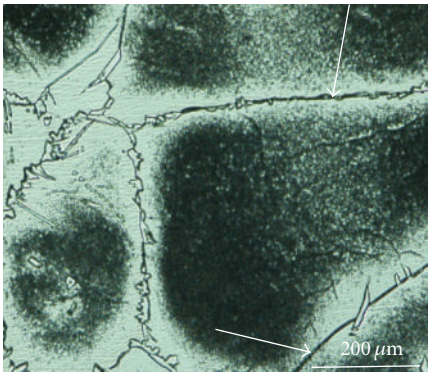

(b) 518 J/mm

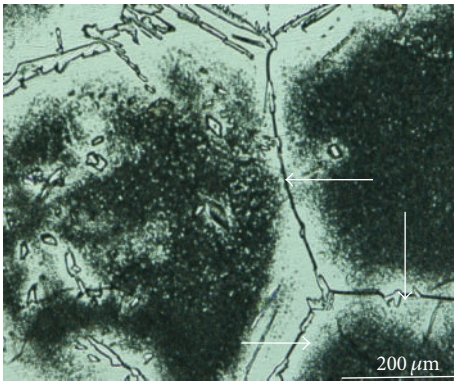

(c) 1296 J/mm

Figure 7: Microstructure of the HTHAZ of cryocooled weld etched electrolytically in 10% oxalic acid.

the influence of the heat input as well as the cooling dynamics. At very low heat input as shown in Figure 5, the cooling rate is high (in the hundreds per minute), the time spent in the dual phase region is short and this reduces the volume fraction of austenite that is formed at elevated temperature.

Therefore, the amount of martensite in the ambient temperature microstructure correspondingly reduces. The resulting ferritic microstructure becomes supersaturated in carbon. The excess carbon in the ferrite is eventually precipitated as chromium carbide essentially on the ferrite-ferrite grain boundary than on the ferrite-martensite grain boundary.

However, as the heat input increases, the cooling rate reduces; this permits transformation within the $\delta + \gamma$ dual phase region and more austenite is formed in the HTHAZ. The austenite absorbs the excess carbon and transforms to martensite at temperatures lower than the Ms point (Figure 2) which is retained down to ambient condition as grain boundary martensite network within a ferritic HTHAZ. This martensite prevents the development of a continuous network of chromium depleted zone in the microstructure. In addition, slower cooling after welding at higher heat input permits the ferrite phase to desensitize through the diffusion of chromium from the interior into any chromium depleted zone [10]. This probably explains the low level of ditched structure observed in the weld made at 1296 J/mm. However, with cryogenic cooling, the cooling rate is about twice that

of conventional welds; and this almost suppresses austenite nucleation and growth as the HTHAZ cools through the $\delta + \gamma$ dual phase field leading to low volume percent of room temperature martensite. This is apparent in Figure 7 which shows a thin network of martensite unlike the network in Figure 6. The low volume percent and thin network of martensite in cryotreated welds encourage higher supersaturation of carbon in the ferrite phase and formation of chromium carbide resulting in chromium depletion and greater ditched structure in the HTHAZ. Furthermore, the high cooling rate associated with cryogenic cooling also prevents the back-diffusion of chromium to the depleted regions adjacent to the chromium-rich carbides. Thus, the level of ditched structure in cryotreated welds is higher than in conventional welds for the same comparative level of heat input.

4. Conclusions

An exploratory study on the influence of cryogenic cooling on the sensitization behaviour in medium chromium ferritic stainless welds has been undertaken. The study established the following.

(i) Low heat input welding condition inhibits austenite formation and encourages the formation of largely ferritic microstructure in the HTHAZ which is prone to chromium carbide precipitation due to supersaturation of carbon in ferrite.

(ii) Martensite content in the HTHAZ region is very critical in evaluating the sensitization behaviour in ferritic stainless steel weld. The HTHAZ with higher martensite content exhibits low level of ditched structure.

(iii) The almost two-fold multiple in cooling rate associated with cryogenic cooling for the same level of heat input restricts the phase transformation within the dual phase region, producing very thin network of martensite. This condition also prevents self-desensitization by inhibiting the diffusion of chromium from the grains interior into any chromium depleted zones. The cryotreated welds invariably exhibit greater ditched structure than conventional welds.

(iv) Though the welds are ditched to different levels, the structure is generally classified as not sensitized since no single grain is completely surrounded by ditches.

Conflict of Interests

The authors declare that there is no conflict of interests regarding the publication of this paper.

Acknowledgment

The authors appreciate facility and technical support from the staff, Non-Destructive Testing, and Tool and Die laboratories, Department of Manufacturing and Materials Engineering, International Islamic University Malaysia, particularly for the provision of liquid nitrogen Dewar for the experimentation on cryogenic cooling.

References

[1] L.-X. Wang, C.-J. Song, F.-M. Sun, L.-J. Li, and Q.-J. Zhai, "Microstructure and mechanical properties of 12 wt.% Cr ferritic stainless steel with Ti and Nb dual stabilization," *Materials and Design*, vol. 30, no. 1, pp. 49–56, 2009.

[2] L. Silva, L. Lima, and W. Campos, "Microstructural characterization of the HAZ of the AISI 439 steel with different heat input," in *Proceedings of the International Nuclear Atlantic Conference*, pp. 1–6, Fortaleza, Brazil, October 2007.

[3] A. Lakshminarayanan, K. Shanmugam, and V. Balasubramanian, "Effect of autogenous arc welding processes on tensile and impact properties of ferritic stainless steel joints," *Journal of Iron and Steel Research International*, vol. 26, no. 1, pp. 62–68, 2009.

[4] J. C. Lippold and D. J. Kotecki, *Welding Metallurgy and Weldability of Stainless Steel*, Wiley-Interscience, Hoboken, NJ, USA, 2005.

[5] M. O. H. Amuda, *Microstructural features of ferritic stainless steel welds [Ph.D. thesis]*, International Islamic University Malaysia, 2008.

[6] V. Balasubramanian, K. Shanmugam, and A. K. Lakshminarayanan, "Effect of autogenous arc welding processes on fatigue crack growth behaviour of ferritic stainless steel joints," *ISIJ International*, vol. 48, no. 4, pp. 489–495, 2008.

[7] D. Carrouge, H. K. D. H. Bhadeshia, and P. Woollin, "Microstructural change in the high- temperature heat affected zone of low-carbon, "13%Cr", martensitic stainless steels," *Stainless Steel World*, pp. 16–23, 2002.

[8] M. W. Warmelo, D. Nolan, and J. Norish, "Mitigation of sensitization effects in unstabilized 12% Cr ferritic stainless steel welds," *Materials Science and Engineering A*, vol. 464, pp. 157–169, 2007.

[9] M. L. Greeff and M. du Toit, "Looking at the sensitization of 11-12% chromium EN 1.4003 stainless steels during welding," *Welding Journal*, vol. 85, no. 11, p. 243s, 2006.

[10] M. du Toit, G. T. Van Rooyen, and D. Smith, "An overview of the heat affected zone sensitization and stress corrosion cracking behavior of 12 % chromium type 1.403 ferritic stainless steel," IIW Doc IX-H-640-06, 2006.

[11] G. M. Reddy and T. Mohandas, "Explorative studies on grain refinement of ferritic stainless steel welds," *Journal of Materials Science Letters*, vol. 20, no. 8, pp. 721–723, 2001.

[12] M. O. H. Amuda and S. Mridha, "A novel scheme for weld microstructure control using cryogenic cooling," *Advanced Materials Research*, vol. 264-265, pp. 343–348, 2011.

[13] E. Folkhard, *Welding Metallurgy of Stainless Steel*, Springer, New York, NY, USA, 1988.

[14] R. H. Kaltenhauser, "Improving the engineering properties of ferritic stainless steels," *Metals Engineering Quarterly*, vol. 11, no. 2, pp. 41–47, 1971.

[15] K. E. Easterling, *Introduction to the Physical Metallurgy of Welding*, Butterworth-Heinemann, Oxford, UK, 2nd edition, 1992.

[16] "Standard practices for detecting susceptibility to intergranular attack in ferritic stainless steel," in *ASTM Annual Book of Standards*, A763-93, pp. 416–426, ASTM International, Dayton, Ohio, USA, 1999.

[17] D. Rosenthal, "Mathematical theory of heat distribution during welding and cutting," *Welding Journal*, vol. 20, no. 5, pp. 220s–234s, 1941.

[18] P. G. H. Pistorius and G. T. van Rooyen, "Composition and properties of ferritic stainless steels with good weldability," *Welding in the World*, vol. 36, no. 1, pp. 65–72, 1995.

[19] M. N. Van Warmelo, *Susceptibility of 12% Cr steels to sensitization during welding of thick gauge plate [M.S. thesis]*, University of Wollongong, New South Wales, Australia, 2006.

[20] A. G. Glover, J. T. McGrath, M. J. Tinkler, and G. C. Weatherly, "The influence of cooling rate and composition on weld metal microstructures in a C/Mn and a HSLA steel," *Welding Journal*, vol. 53, no. 9, pp. 267s–273s, 1977.